Development of Mastoid Air Cell System Extraction Method on Temporal CT-scan Image

Syafri Arlis[1], Sarjon Defit[2], Sumijan[3]
[1]Information Systems, Faculty of Computer Science, Universitas Putra Indonesia YPTK
[2,3]Information Technology, Faculty of Computer Science, Universitas Putra Indonesia YPTK
[1]syafri_arlis@upiyptk.ac.id, [2]sarjon_defit@upiyptk.ac.id, [3]sumijan@upiyptk.ac.id

Abstract

Mastoiditis is disease that to infection of the mastoid bone cavity that affects the size of the air cell system of the temporal bone. Visually, the information temporal CT image mastoid bone has can assist medical experts in viewing the mastoid air cell system (MACS), but the fact that medical personnel are experiencing difficulties in determining the size MACS is due to the many different characteristics and objects overlap, so that in the measurement of the area, precise and accurate results have not been obtained. This study aims to separate the object of the MACS with the development of extraction. The proposed method uses Morphology and Regionprops operations. The dataset used in the testing process is 347 of 5 patients indicated for Mastoiditis. The results obtained can calculate the area of MACS for each test image. Based on image testing, the area of the smallest MACS in this study was 0.589 cm^2 and the largest was 6.183 cm^2. This, the smaller the size of the MACS indicates the severity of infection, so this study can help medical personnel make decisions and take appropriate treatment actions.

Keywords: image extraction, mastoid air cell system, morphology, regionprops

1. Introduction

Image processing aims to manipulate images and the process of retrieving information from the results of image pattern analysis with the help of computer media to detect objects [1,2]. Medical image processing has a very important role in clinical diagnosis, such as in surgery, treatment planning and evaluation, then prediction of the development of a disease. The development of medical imaging information technology can be obtained quickly such as by using computed tomography (CT). CT-scan is a medical imaging method that has high resolution and contrast that can be used to recognize and evaluate small features of the middle ear, inner ear, mastoid process and base of the cranium. [3]. The results of this image provide an overview of the anatomy of the organ that can be used by radiologists to measure organs or identify abnormal parts [4].

Mastoiditis occurs due to the expansion of inflammation of the middle ear, where the result of this inflammation affects the size of the mastoid air cells [5]. This infection can spread from the temporal bone to the head and neck making it difficult and necessitating cross-sectional imaging in diagnosing and planning surgery [6,7]. In the medical field, misdiagnosis or the absence of a specialist can affect a patient's health, lead to unnecessary testing and increase health care costs. In particular, the lack of otolaryngology specialists forces patients to seek medical attention from general practitioners, who may not have sufficient training and experience to make a correct diagnosis[8]. To overcome this problem the application of a computer-aided system based on CT-scan image processing techniques for examination and as support for more accurate diagnosis [9].

Diagnosis of Mastoiditis the patient must perform a medical examination using a combination of X-ray technology. The results of this X-ray image are in the form of a CT-scan or an MRI scan of the Temporal bone. The mastoid bone is located behind the temporal bone. Imaging examination aims to determine abnormalities in the Temporal bone which can be done with photos or by looking at the results of CT-scan or Magnetic Resonance Imaging (MRI) examination images [10,11]. Medical experts diagnose this disease Mastoiditis by looking at the air cells contained in the image of the cavity of the Temporal bone resulting from the acquisition of a CT-scan or MRI and given to a doctor for analyze and further medical action [12]. The

shape of the CT-scan or MRI image results can be seen in Figure 1.
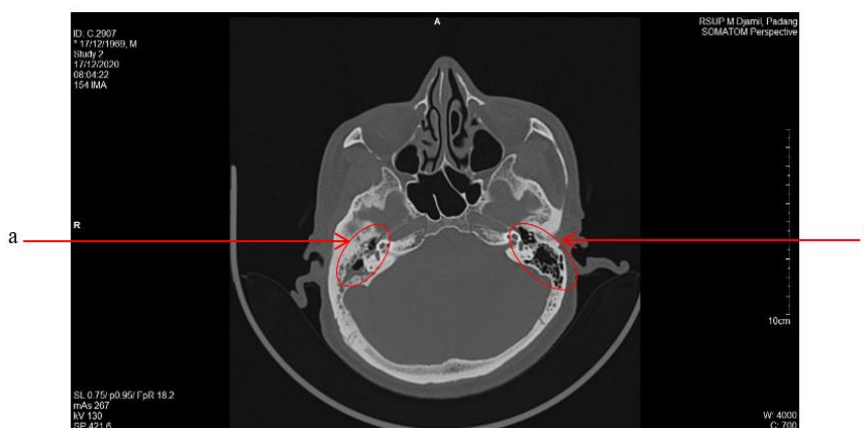

Figure 1. Mastoid Air Cell System on Axial CT Temporal Section, (a). Right Area, (b). Left Area

Visually, the information on the Temporal CT-scan can help doctors determine the area of the mastoid air cell system (MACS), but it is still difficult to determine the area of the MACS. This problem focuses on a number of overlapping objects making it difficult to measure the area of the MACS [13]. For this reason, a more precise and accurate analysis is needed to assist surgeons and doctors in the process of calculating the area of the MACS by performing an automatic extraction to separate the right and left areas of the air cell system on a Temporal bone CT-scan.

The application of information technology in image processing to identify the MACS has been carried out in previous studies. The process of extracting the size of the MACS around the ear using Image Filtering, Image Enhancement and Feature Extraction methods produces excellent accuracy and the speed of the proposed method is tested on low-resolution CT-scan images automatically compared to manual segmentation [14,15]. Furthermore, the same study explained that the extraction process on mastoid objects using Feature Region, Multilevel Otsu and Morphology on Temporal bone CT-scan was able to identify air cell system objects [16,17]. Furthermore, the automatic extraction process on the micro part of the Temporal bone structure from the CT-scan image with the Morphological Enhancement and Convolutional Neural Network (CNN) methods produces an accurate detection of the Temporal bone structure [18]. In another study, it was explained that the segmentation and extraction process using the Convolutional Neural Network (CNN) method combined with the Region Extraction method gave limited results in the middle ear and did not focus on the MACS [19].

Modern medical imaging technology helps surgeons get a picture of the structure of the ear. In supporting the implementation of surgery, image extraction is needed to determine the structure of the surrounding image objects, so as to increase the success of the operation. This study developed an image extraction method that aims to separate the MACS in both ear cavities, both right ear cavity and left ear cavity on axial CT-scan of Temporal bone. The novelty of this study presents the extraction process in separating objects from the MACS without changing the pixel size of each test image. These results are able to obtain objects to be analyzed and used to calculate the size of the area of the MACS and the size based on the severity of the infection.

2. Research Method

The stages in this research consist of image input, image cropping, image quality improvement with median filter, followed by conversion to binary image. Furthermore, the results of the binary image are extracted using the MACS. The research stages are shown in Figure 2.
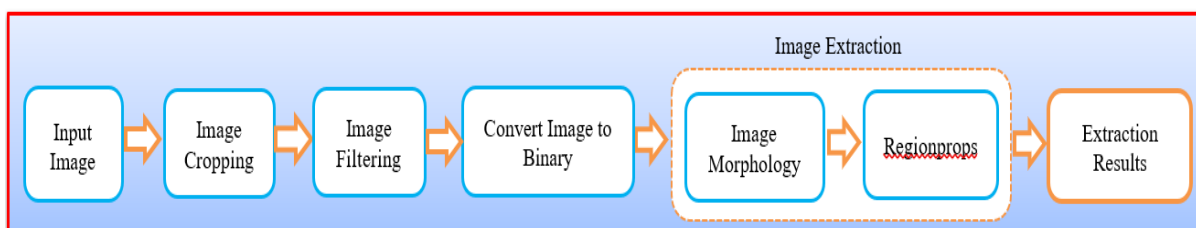

Figure 2. Research Stages

2.1 Input Image

The input image data used for testing is sourced from M. Djamil Hospital, Padang, West Sumatra, Indonesia. Image taken through a CT-scan of the head, especially the axial section of the Temporal bone. Image retrieval using a CT-scan tool Siemens SOMATOM Perspective CT Scanner with specifications X-ray Tube Dura 688-MV model 10662260 with conversion value per pixel = 0.29 mm. The CT-scan results are visualized with the syngo® fastView application and converted and saved in the form of a digital image with the Joint Photographic Group (JPG) format in grayscale. The number of data tested is 12 (twelve) patients. Each patient consists of multiple slices with 64-slice and 128-slice configurations. In each slice of the image there is some information such as the name of the hospital, the type of CT device, the patient's name, the patient's date of birth, the date the CT-scan was performed, the acquisition parameter (mAs), the tube voltage value (kV), the width and width and the size of each slice. in every pixel.

2.2 Image Cropping

The cropping process aims to eliminate unnecessary noise outside the object of research by cutting each side of the object and removing areas that are not needed [20]. The results of this cut will get the area that will be needed so that the area that is not needed that is outside the area of the object of the Region of Interest (ROI) being studied can be removed [21].

2.3 Image Filtering

The image filtering process aims to eliminate some variation in values between neighboring pixels that can interfere with the quality of the input image and to adjust the pixel value to the Histogram Level value [22], thereby improving image quality so that it can be processed at a later stage. Equation 1 is the formula used to perform the Median Filtering process.

$$\ddot{fm}(\text{H},\text{k}) = median_{(\text{i},\text{j})\in k_{H,k}}\left\{g(\text{i},\text{j})\right\} \qquad (1)$$

Where $\ddot{fm}(\text{H},\text{k})$ is the result of median filter, $(\text{i},\text{j}) \in k_{H,k}$ are the coordinates of the filter and $g(\text{i},\text{j})$.

The image filtering process can be presented in the Algorithm 1.

2.4 Binary Image Conversion

Image conversion process by changing from color image or gray scale image to binary image for the purpose of image segmentation. Image segmentation aims to separate objects, so we need the right segmentation method. The segmentation method used is the threshold value method in recognizing the image with the aim of converting it to a binary image [23]. The

image resulting from the filtering process is converted into a binary image with the threshold value method that has been developed with the extended Adaptive Global Threshold (eAGT) to calculate the optimal threshold value for each input image to be studied automatically, which is presented in the Algorithm 2.

```
Algorithm 1: Median filtering Process
Start
Read the Cropped Image Image =Img
Show Image Image
Initialization of Histogram H and Starting
Point
for i = 1 to M do
for j = 1 to N do
for k=-n/2 to n/2 do
Delete Img_{i+k,j-n/2-1} from H
add Img_{i+k,j+n/2-1} for H
update k
end for
Y_{i,j←median(H,k)}
end for
end for
Finish
```

2.4 Binary Image Conversion

Image conversion process by changing from color image or gray scale image to binary image for the purpose of image segmentation. Image segmentation aims to separate objects, so we need the right segmentation method. The segmentation method used is the threshold value method in recognizing the image with the aim of converting it to a binary image [23]. The image resulting from the filtering process is converted into a binary image with the threshold value method that has been developed with the extended Adaptive Global Threshold (eAGT) to calculate the optimal threshold value for each input image to be studied automatically, which is presented in the Algorithm 2.

```
Algorithm 2. extended Adaptive Global
Threshold (eAGT)
Function unique, imhist
Input: Im(m,n)
        Initialization
        [m,n,l] = size(Im)
        aAGT, i = 0
        IntensitasLevel = unique (Im)
        [px, gL] = imhist (Im (Im >= i), i)
        aAGT = find (px / IntensitasLevel)
Output: eAGT
```

2.5 Image Extraction

The image extraction process aims to separate the ROI area from the background, so as to obtain information and distinguishing characteristics of the object to be analyzed [24,25]. The obstacle in the image extraction process is how to separate the desired object from several objects in the image that have the same intensity value, especially in this study the many characteristics of the object and overlapping in the Temporal bone image with the same intensity value. To extract the desired object, it is necessary to separate each binary

value of the object in the image by calculating the ratio of the perimeter values of each object [26].

2.5.1 Operation Morphology

Morphological operations aim to analyze the shape of the object from an image and separate the required area and extract the structure and shape of the image [27]. The extraction process uses Closing Morphology involving several images that have been previously processed and Element Structure (Strel) which aims to remove small areas and smooth out contours [28]. Equation 2 presents the Morphological Closing formula.

$$A \bullet B = (A \oplus B)\Theta B \qquad (2)$$

with morphological operations A against B is the dilation of A by B followed by erosion of the result with B.

2.5.2 Regionprops Method

The results of the image extraction process using the morphological method are then labeled for each matrix area using the Regionprops method. Regionprops detects white objects with a pixel value of 1 and black objects with a pixel value of 0 as the background [29]. Representation of the Regionprops area with an elliptical approach is presented in Figure 3

Figure 3. Representation of Regionprops with Elliptical Approximation

3. Result and Discussion

In this study, only one slice of the image will be tested for each axial CT-scan Temporal image that is clearly visible for patients with Mastoiditis. Seen on the left, the mastoid air cells are still shaped and normal, characterized by a honeycomb-like partitioned appearance and black in color, while the right inner ear canal is not shaped, due to infection or inflammation in the mastoid area. The test image is 1275 x 727 pixels in JPG format in grayscale, as shown in Figure 4.
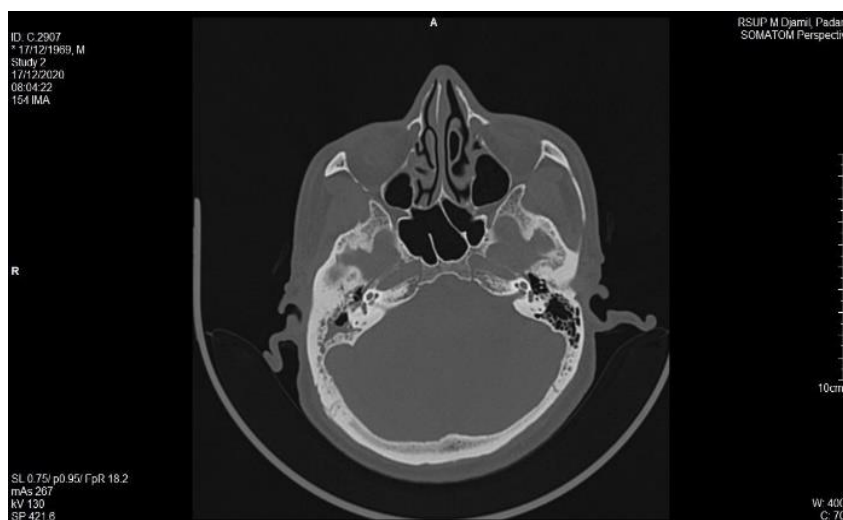

Figure 4. Input Image Temporal CT

Next, the input image is subjected to an image cropping process to remove unnecessary information and determine exactly what part of the image is that contains the object area to be analyzed, so that it can be separated from areas that are not needed for further processing. The results of this process are presented in Figure 5, where significant changes have been made by eliminating some unnecessary information and objects can be identified.

After the image cropping process is carried out, the next step is to carry out the image quality improvement process with the aim of eliminating small variations between neighboring pixels that can interfere with the quality of the input image and adjusting the value of each pixel to the histogram value level, thereby improving image quality and eliminating noise for processed at a later stage. Image enhancement results are shown in Figure 6.
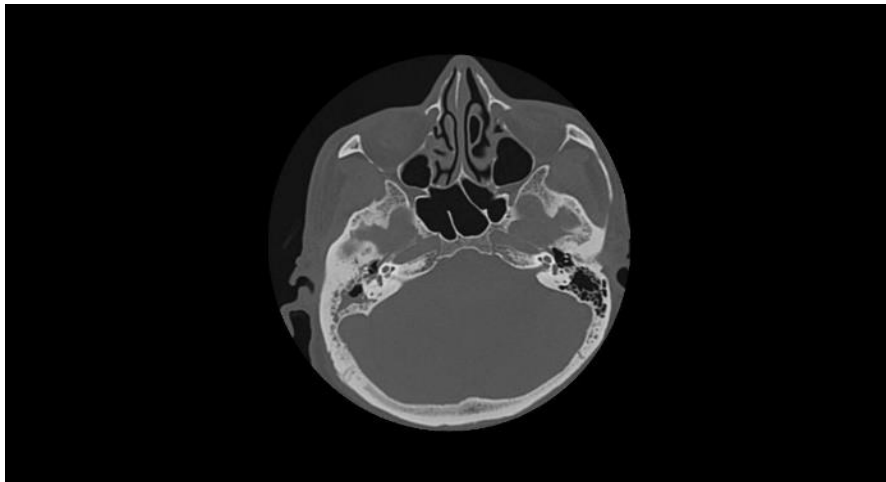
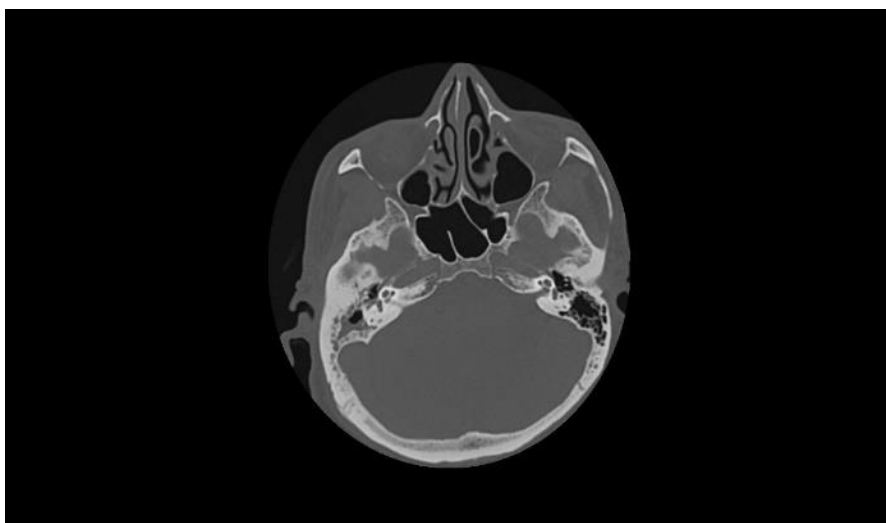Figure 5. The Result of the Image Cropping Process

Figure 6. Image Filtering Results

The next step is to convert the image from the image filtering results into a binary image. This stage performs the image conversion process using the eAGT method which was developed to obtain the optimal threshold value for each tested image by calculating the number of pixel intensities from the normalized histogram and the number of unique values of different pixel intensities based on the color intensity level, due to the large number of object features. found in the CT image of the temporal bone. The results of this segmentation still have areas or objects that are not needed. Next remove noise by removing unneeded objects and emphasizing objects to be identified, as depicted in Figure 7.

Figure 7. Image Segmentation Process Results, (a) Binary Image, (b) Object identification

The image presented in figure 7(b) has removed noise and unneeded areas and there is only an area of the MACS to be extracted with the aim of separating the right and left areas of the MACS by morphological operations and further separating the areas of objects that are calculate perimeter values and distances between pixels with the Regionprops command. The results of this process are depicted in Figure 8.
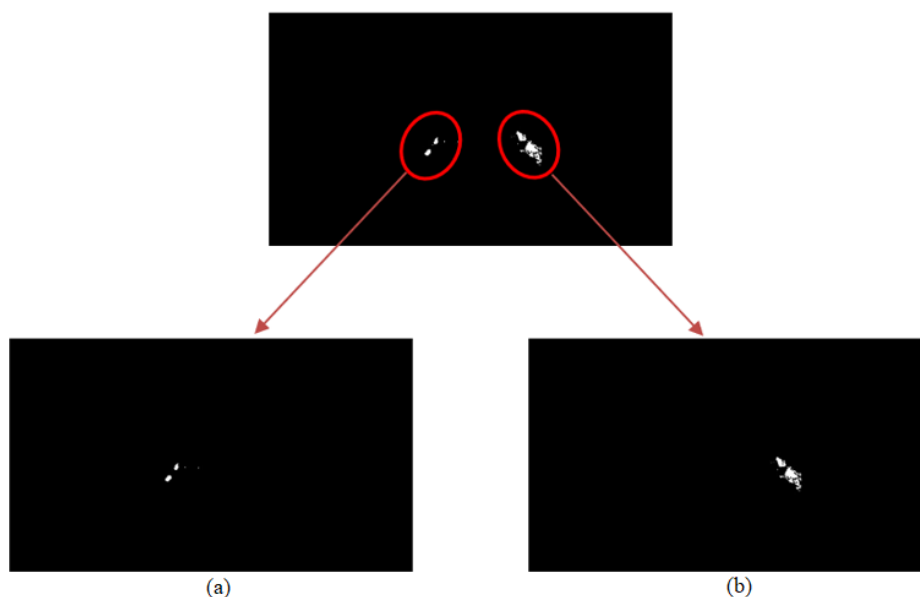

Figure 8. MACS Extraction Results, (a) Right Area, (b) Left Area

Temporal image of axial sections in patients who have been extracted, there is an area of the MACS that is still normal, namely in the area on the left, while on the right it cannot identify the presence of the MACS, this is because there is a space in the MACS in the hole. Ear shrinkage caused by the area around the mastoid cavity experiencing an infection. The MACS that has been extracted automatically is then calculated for the pixel area. Furthermore, this pixel area will be used to calculate the area of the extracted area automatically, so that the area is obtained, where the size of each pixel = 0.29 mm and this result is converted into square centimeters (cm2). The results of the extraction and calculation of the area of the MACS are presented in Table 1.

Table 1. MACS Extraction Results

Slice-	MACS Identification	Binary Image with eAGT Method	MACS Extraction	
			Right Area	Left Area
Slice 1				
Slice 2				
Slice 3				

Slice 4

Slice 5

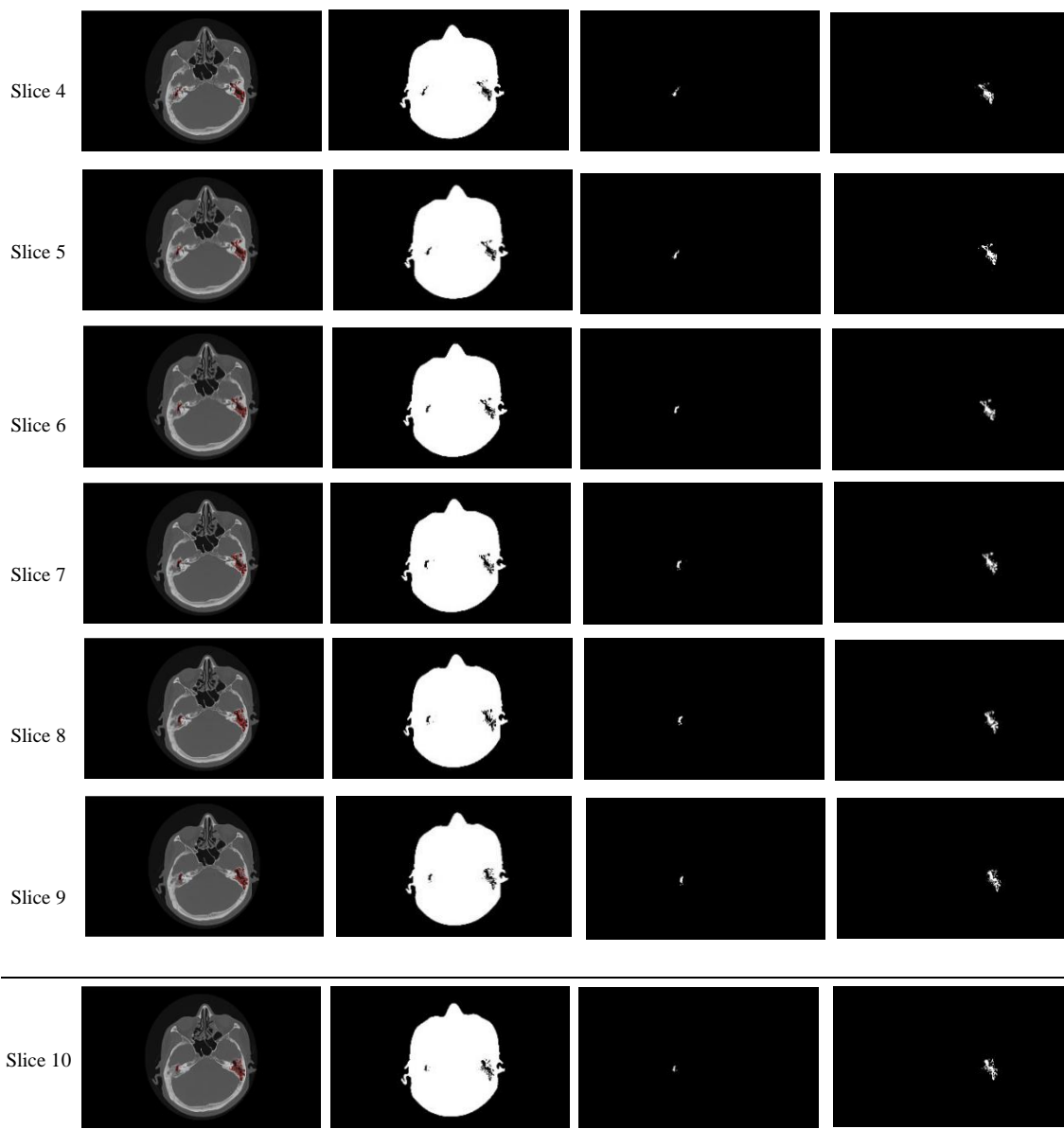Slice 6

Slice 7

Slice 8

Slice 9

Slice 10

Table 1 shows the extraction results of the MACS. The results of this extraction are used to calculate the pixel area of the MACS object on the Mastoid CT-scan image. The results of the pixel area and the measurement of the area of the m can be seen in Table 2.

Table 2. Calculation of the Area of MACS

Slice to-	Pixel Area		Area (cm²)	
	Right Area	Left Area	Right Area	Left Area
Slice 1	470	2132	1,363	6,183
Slice 2	344	1712	0,998	4,965
Slice 3	320	1689	0,928	4,898
Slice 4	348	1836	1,009	5,324
Slice 5	368	1927	1,067	5,588
Slice 6	342	1837	0,992	5,327
Slice 7	388	1889	1,125	5,478
Slice 8	385	1972	1,117	5,719
Slice 9	326	1896	0,945	5,498
Slice 10	203	1860	0,589	5,394

Based on the discussion above, that this study provides results that can separate objects from the MACS, both in the right and left areas on Temporal CT. This result is also supported by the obtained pixel area, the area of each object area of the MACS which is separated in each test image. The smallest pixel area of this research

is 203 pixels and the largest is 2132 pixels. Furthermore, this pixel area is used to calculate the area extracted automatically, where the smallest area of the MACS is 0.589 cm^2 and the largest area is 6.183 cm^2. With these results, the development of the extraction method by applying Morphological operations and the Regionprops method is able to provide optimal results compared to other extraction methods. So that the results of this study can help medical personnel in taking further action.

4. Conclusion

The results of the Temporal CT-scan image processing of patients with Mastoiditis, obtained the results of the extraction of the MACS, both the right area and the left area automatically. The results of this extraction are used to calculate the area of the MACS in the ear cavity. The smallest pixel area of this research is 203 pixels and the largest is 2132 pixels. Furthermore, the smallest area of the MACS is 0.589 cm^2 and the largest area is 6.183 cm^2. With these results, it can be concluded that the smaller the area of the MACS indicates the occurrence of inflammation in the Mastoid area, so the results of this study can be used as recommendations and referrals for doctors in making decisions and taking appropriate treatment actions.

Reference

[1] Yuhandri, S. Madenda, E. P. Wibowo, and karmila@staff gunadarma ac id Karmilasari, "Object feature extraction of songket image using chain code algorithm," *Int. J. Adv. Sci. Eng. Inf. Technol.*, vol. 7, no. 1, pp. 235–241, 2017, doi: 10.18517/ijaseit.7.1.1479.

[2] M. Yasir, M. S. Hossain, S. Nazir, S. Khan, and R. Thapa, "Object Identification Using Manipulated Edge Detection Techniques," *Science (80-.).*, vol. 3, no. 1, pp. 1–6, 2022, doi: 10.11648/j.scidev.20220301.11.

[3] H. Rodrigues *et al.*, "*Mastoid*, middle ear and inner ear analysis in *CT-scan* – a possible contribution for the identification of remains," *Med. Sci. Law*, vol. 60, no. 2, pp. 102–111, 2020, doi: 10.1177/0025802419893424.

[4] L. Liu, J. Cheng, Q. Quan, F. X. Wu, Y. P. Wang, and J. Wang, "A survey on U-shaped networks in medical image segmentations," *Neurocomputing*, vol. 409, pp. 244–258, 2020, doi: 10.1016/j.neucom.2020.05.070.

[5] N. Bartov *et al.*, "Management of Acute *Mastoiditis* with Immediate Needle Aspiration for Subperiosteal Abscess," *Otol. Neurotol.*, vol. 40, no. 6, pp. E612–E618, 2019, doi: 10.1097/MAO.0000000000002231.

[6] M. W. Mather, P. D. Yates, J. Powell, and I. Zammit-Maempel, "Radiology of acute *Mastoiditis* and its complications: A pictorial review and interpretation checklist," *J. Laryngol. Otol.*, vol. 133, no. 10, pp. 856–861, 2019, doi: 10.1017/S0022215119001609.

[7] D. H. Toneva, S. Y. Nikolova, D. K. Zlatareva, V. G. Hadjidekov, and N. E. Lazarov, "Sex estimation by *Mastoid* Triangle using 3D models," *Homo*, vol. 70, no. 1, pp. 63–73, 2019, doi: 10.1127/homo/2019/1010.

[8] M. Viscaino, J. C. Maass, P. H. Delano, M. Torrente, C. Stott, and F. Auat Cheein, "Computer-aided diagnosis of external and middle ear conditions: A machine learning approach," *PLoS One*, vol. 15, no. 3, pp. 1–18, 2020, doi: 10.1371/journal.pone.0229226.

[9] Q. Nie, Y. bing Zou, and J. C. W. Lin, "Feature Extraction for Medical CT Images of Sports Tear Injury," *Mob. Networks Appl.*, vol. 26, no. 1, pp. 404–414, 2021, doi: 10.1007/s11036-020-01675-4.

[10] H. A. Balfas, *No Title*, Bedah Otol. Bedah Otologi Dan Bedah Neutrologi Dasar, 2017.

[11] H. S. Gendeh, A. binti Abdullah, B. S. Goh, and N. D. Hashim, "Intracranial Complications of Chronic Otitis Media: Why Does It Still Occur?," *Ear, Nose Throat J.*, vol. 98, no. 7, pp. 416–419, 2019, doi: 10.1177/0145561319840166.

[12] N. R. Sayal, S. Boyd, G. Zach White, and M. Farrugia, "Incidental *Mastoid* effusion diagnosed on imaging: Are we doing right by our patients?," *Laryngoscope*, vol. 129, no. 4, pp. 852–857, 2019, doi: 10.1002/lary.27452.

[13] S. W. Byun, S. S. Lee, J. Y. Park, and J. H. Yoo, "Normal *Mastoid* air cell system geometry: Has surface area been overestimated?," *Clin. Exp. Otorhinolaryngol.*, vol. 9, no. 1, pp. 27–32, 2016, doi: 10.21053/ceo.2016.9.1.27.

[14] O. Cros, M. Gaihede, A. Eklund, and H. Knutsson, "Surface and curve skeleton from a structure tensor analysis applied on *Mastoid* air cells in human *Temporal* bones," *Proc. - Int. Symp. Biomed. Imaging*, vol. i, pp. 270–274, 2017, doi: 10.1109/ISBI.2017.7950517.

[15] S. Nikan *et al.*, "Pwd-3dnet: A deep learning-based fully-automated segmentation of multiple structures on *Temporal* bone ct scans," *IEEE Trans. Image Process.*, vol. 30, pp. 739–753, 2021, doi: 10.1109/TIP.2020.3038363.

[16] Z. Liu, C. Maere, and Y. Song, "Novel approach for automatic region of interest and seed point detection in CT images based on *Temporal* and spatial data," *Comput. Mater. Contin.*, vol. 59, no. 2, pp. 669–686, 2019, doi: 10.32604/cmc.2019.04590.

[17] K. A. Powell, T. Kashikar, B. Hittle, D. Stredney, T. Kerwin, and G. J. Wiet, "Atlas-based segmentation of *Temporal* bone surface structures," *Int. J. Comput. Assist. Radiol. Surg.*, vol. 14, no. 8, pp. 1267–1273, 2019, doi: 10.1007/s11548-019-01978-2.

[18] Y. Lv, J. Ke, Y. Xu, Y. Shen, J. Wang, and J. Wang, "Automatic segmentation of *Temporal* bone structures from clinical conventional CT using a CNN approach," *Int. J. Med. Robot. Comput. Assist. Surg.*, vol. 17, no. 2, pp. 1–9, 2021, doi: 10.1002/rcs.2229.

[19] R. Hussain, A. Lalande, K. B. Girum, C. Guigou, and A. Bozorg Grayeli, "Automatic segmentation of inner ear on *CT-scan* using auto-context convolutional neural network," *Sci. Rep.*, vol. 11, no. 1, pp. 1–10, 2021, doi: 10.1038/s41598-021-83955-x.

[20] K. U. Ahamed *et al.*, "A deep learning approach using effective preprocessing techniques to detect COVID-19 from chest *CT-scan* and X-ray images," *Comput. Biol. Med.*, vol. 139, no. October, p. 105014, 2021, doi: 10.1016/j.compbiomed.2021.105014.

[21] L. J. Jensen, D. Kim, T. Elgeti, I. G. Steffen, B. Hamm, and S. N. Nagel, "Stability of radiomic features across different region of interest sizes-A CT and MR phantom study," *Tomography*, vol. 7, no. 2, pp. 238–252, 2021, doi: 10.3390/tomography7020022.

[22] J. Na'am *et al.*, "Detection of infiltrate on infant chest X-ray," *Telkomnika (Telecommunication Comput. Electron. Control.*, vol. 15, no. 4, pp. 1943–1951, 2017, doi: 10.12928/TELKOMNIKA.v15i4.3163.

[23] Katherine, R. Rulaningtyas, and K. Ain, "*CT-scan* image segmentation based on hounsfield unit values using Otsu thresholding method," *J. Phys. Conf. Ser.*, vol. 1816, no. 1, 2021, doi: 10.1088/1742-6596/1816/1/012080.

[24] A. Soni and A. Rai, "*CT-scan* Based Brain Tumor Recognition and Extraction using Prewitt and Morphological Dilation," *2021 Int. Conf. Comput. Commun. Informatics, ICCCI 2021*, vol. 1, no. 1, 2021, doi: 10.1109/ICCCI50826.2021.9402677.

[25] R. I. Borman, Y. Fernando, Y. Egi, and P. Yudoutomo, "Identification of Vehicle Types Using Learning Vector Quantization," vol. 5, no. 158, pp. 339–345, 2022, doi: 10.29207/resti.v6i2.3954

[26] eman samir, E. S. Sabry, F. E. A. El-Samie, S. Elagooz, G. El

Banby, and R. A. Ramadan, "Evaluating Image Extraction Methods Over Different Types of Images," *SSRN Electron. J.*, pp. 1–14, 2022, doi: 10.2139/ssrn.4024192.

[27] A. Loddo, C. Di Ruberto, and M. Kocher, "Recent advances of malaria parasites detection systems based on mathematical morphology," Sensors (Switzerland), vol. 18, no. 2, pp. 1–21, 2018, doi: 10.3390/s18020513.

[28] Sumijan, S. Madenda, J. Harlan, and E. P. Wibowo, "Hybrids Otsu method, feature region and mathematical morphology for calculating volume hemorrhage brain on *CT-scan* image and 3D reconstruction," *Telkomnika (Telecommunication Comput. Electron. Control.*, vol. 15, no. 1, pp. 283–291, 2017, doi: 10.12928/TELKOMNIKA.v15i1.3146.

[29] Na'am, J., Pranata, F. S., Hidayat, R., Adif, A. M., & Ellyzarti, E. (2021). Automated Identification Model of Ground-Glass Opacity in CT-Scan Image by COVID-19. International Journal on Advanced Science, Engineering and Information Technology, 11(2), 595-602, doi:10.18517/ijaseit.11.2.14143.